

Cooling Flows and Radio Mini-Halos in Clusters of Galaxies

Myriam Gitti,^{1,2,3} Gianfranco Brunetti,³ Giancarlo Setti,^{2,3} and Luigina Feretti³

¹ *Institute of Astrophysics, University of Innsbruck, Technikerstraße 25, A-6020 Innsbruck, Austria*

² *Dipartimento di Astronomia, Università di Bologna, via Ranzani 1, I-40127 Bologna, Italy*

³ *Istituto di Radioastronomia del CNR, via Gobetti 101, I-40129 Bologna, Italy*

We apply to radio mini-halo candidates a model for electron re-acceleration in cooling flows (Gitti, Brunetti, & Setti 2002). In agreement with the basic idea of the model, we find that the power required for the re-acceleration of the electron population is only a small fraction of the maximum power that can be extracted from the cooling flow (as estimated on the basis of the standard model). Observationally, we notice that the strongest radio mini-halos are found in association with the most powerful cooling flows, and that cooling flow powers are orders of magnitude larger than the integrated radio power. Possible effects of new *Chandra* and *XMM-Newton* estimates of \dot{M} on this trend are considered: we conclude that even if earlier derived cooling rates were overestimated, cooling flow powers are still well above the radio powers emitted by mini-halos.

1. Introduction

It is well known that the radio emission from clusters of galaxies generally originates from individual radio emitting galaxies. In addition, some clusters of galaxies show synchrotron emission not directly associated with a particular galaxy but rather diffused into the intracluster medium (ICM). These diffuse radio sources, which are the most spectacular probe of the existence of non-thermal emission from the ICM, have been classified in three classes: cluster-wide halos, relics and mini-halos (Feretti & Giovannini 1996). Both cluster-wide halos and relics have low surface brightness, large size (~ 1 Mpc) and steep spectrum, but the former are located at the cluster centers and show low or negligible polarized emission, while the latter are located at the cluster peripheries and are highly polarized. The diffuse radio emission is found in clusters which show significant evidence for an ongoing merger (e.g. Edge, Stewart & Fabian 1992; Giovannini & Feretti 2002). It was proposed that recent cluster mergers may play an important role in the re-acceleration of the radio-emitting relativistic particles, thus providing the energy to these extended sources (e.g. Tribble 1993; Brunetti et al. 2001). The merger picture is consistent with the occurrence of large-scale radio halos in clusters without a cooling flow, since the major merger event is expected to disrupt a cooling flow (e.g. Sarazin 2002 and references therein).

Mini-halos are diffuse radio sources, extended on a smaller scale (up to ~ 500 kpc), surrounding a dominant radio galaxy at the cluster center. They are only observed in clusters with a cooling flow and it has been found that these sources are not connected to ongoing cluster merger activity. Their radio emission is indicative of the presence of diffuse relativistic particles and magnetic fields in the ICM, since these sources do not appear as extended lobes maintained by an Active Galactic Nucleus (AGN), as in classical radio galaxies (Giovannini &

Feretti 2002).

More specifically, Gitti, Brunetti, & Setti (2002, hereafter GBS) suggested that the diffuse synchrotron emission from radio mini-halos is due to a relic population of relativistic electrons re-accelerated by MHD turbulence via Fermi-like processes, with the necessary energetics supplied by the cooling flow. Very recently, the alternative possibility of hadronic origin for radio mini-halos has also been discussed (Pfrommer & Enßlin 2003).

Here, we present the application of GBS's model to radio mini-halo candidates and discuss the observational properties of the population of radio mini-halos.

In particular, in Sect. 2 we briefly review GBS's model, and in Sect. 3 we present the application of the model to the Perseus cluster and to the new mini-halo candidate A2626, and discuss the results. In Sect. 4 we present the observational properties of radio mini-halo candidates in relation to those of host clusters.

A Hubble constant $H_0 = 50 \text{ km s}^{-1} \text{ Mpc}^{-1}$ is assumed. The radio spectral index α is defined such as $S_\nu \propto \nu^{-\alpha}$ and, where not specified, all the formulae are in cgs units.

2. Model for the Origin of Radio Mini-Halos

The spatial extent of the diffuse radio emission from mini-halos represents a serious problem for understanding the origin of these sources. The radiative lifetime of an ensemble of relativistic electrons losing energy by synchrotron emission and inverse Compton (IC) scattering off the CMB photons is given by:

$$\tau_{\text{sin+IC}} \simeq \frac{24.5}{[(B^2 + B_{\text{CMB}}^2)\gamma]} \text{ yr} \quad (1)$$

where B is the magnetic field intensity (in G), γ is the Lorentz factor and $B_{\text{CMB}} = 3.18 \times 10^{-6}(1+z)^2$ G is the magnetic field equivalent to the CMB. In a cooling flow region (i.e. for distances $r < r_c$, the cooling radius) the compression of the thermal ICM is expected

to produce a significant increase of the strength of the frozen-in cluster magnetic field and consequently of the electron radiative losses. Therefore, in the absence of a re-acceleration or continuous injection mechanisms, relativistic electrons injected at a given time in these strong fields (of order of 10–20 μG , Ge & Owen 1993; Carilli & Taylor 2002) should already have lost most of their energy and the radio emission would not be observable for more than $\sim 10^7$ – 10^8 yr. Such a radiative lifetime is orders of magnitude shorter than the characteristic diffusion time necessary for the radio-emitting electrons to cover the distance on which the diffuse radio emission from mini-halos is observed, therefore it is plausible that some re-acceleration mechanisms able to balance the radiative losses and modify the electron energy spectrum is acting.

In order to evaluate the radiative losses in the cooling flow region at any distance from the cluster center it is necessary to parameterize the radial dependence of the field strength, which depends on the compression of the thermal gas in the cooling region (i.e., on $n(r/r_c)$, r_c being the cooling radius). On the one hand, the X-ray emission and the spectra of cooling flow clusters unavoidably show the increase of the gas density and the decrease of the temperature towards the center of these clusters. On the other hand, *Chandra* and *XMM-Newton* observations have pointed out that the mass deposition rates in cooling flows have been overestimated in the past by a factor 5–10 (e.g. Fabian & Allen 2003); the new mass deposition rates are not too different from the masses of cold gas estimated by the recent IRAM observations (Edge 2001; Salomé & Combes 2003). In addition, high spectral resolution observations with the Reflection Grating Spectrometer (RGS) on *XMM-Newton* do not show evidence for gas cooling at temperature lower than 1–2 keV (e.g. Peterson et al. 2003).

All these studies basically confirm the idea that the gas cools and thus is compressed in the central region of the cooling cores. On the other hand, they also point out that the physics of the ICM in these regions is more complex than that described by the standard cooling flow models. Unfortunately, no successful model in alternative to the standard model has been proposed yet. Therefore, as a first approximation in our model calculations, we will evaluate the radial behaviour of the physical quantities in the ICM making use of the standard, i.e. single phase, cooling flow model.

In the framework of this model, the increase of the strength of the frozen-in cluster magnetic field is $B \propto r^{-2}$ for radial compression (Soker & Sarazin 1990) or $B \propto r^{-0.8}$ for isotropic compression (Tribble 1993).

The time evolution of the energy of a relativistic electron in these regions is determined by the competing processes of losses and re-accelerations (both related to the magnetic field):

$$\dot{\gamma}(x) = -\beta(x)\gamma^2(x) + \alpha_+(x)\gamma(x) - \chi(x) \quad (2)$$

where $x = r/r_c$, β is the coefficient of synchrotron and IC losses, α_+ the re-acceleration coefficient and χ the Coulomb loss term.

The main assumption of GBS’s model is that a relic

population of relativistic electrons (originated for example in a central active galaxy and then spread throughout the whole cooling flow region by diffusion in few Gyr) as well as a seed large-scale turbulence (naturally originated in the ICM for example as a result of past merger events or motion of the galaxies in the cluster, or due to the interaction of the radio lobes of the central galaxy with the cooling flow itself), are present in the cooling flow region, and that the relic electrons can be efficiently re-accelerated via Fermi-like processes by magnetohydrodynamic (MHD) turbulence amplified by the compression of the magnetic field in the cooling flow region. However, the turbulence must not be too high in order to avoid the disruption of the cooling flow: this fine tuning of the turbulent energy could explain, at least qualitatively, the rarity of these radio sources.

In the present paper, we consider a coefficient for systematic re-acceleration given by (Melrose 1980)

$$\alpha_+(x) \approx (\pi/c) v_A^2(x) l^{-1}(x) [\delta B(x)/B(x)]^2 \quad (3)$$

where $v_A = \sqrt{B^2/4\pi\rho}$ is the Alfvén velocity, and l is the characteristic MHD turbulence scale. For simplicity we assume $\delta B(x)/B(x) = \text{const}$. The energy at which the losses are balanced by the re-acceleration, γ_b , is obtained by Eq. 2 and, since Coulomb losses are nearly negligible at such electron energies, it is $\gamma_b \approx \alpha_+/\beta$.

Under these assumptions, the stationary spectrum of the relativistic electrons is given by (Gitti et al. 2003)

$$N(\gamma, x) \approx N(\gamma_b)_c \left(\frac{\gamma_{b,c}}{\gamma_b(x)} \right)^2 e^2 x^{-s} \cdot \left(\frac{\gamma}{\gamma_b(x)} \right)^2 e^{(-2\gamma/\gamma_b(x))} \quad (4)$$

which is essentially peaked at γ_b and where the electron energy density has been parameterized as $\propto x^{-s}$, s being a free parameter. The other free parameters are $B_c = B(r_c)$ and $l_c = l(r_c)$.

3. Model application to observed mini-halos

In this section we will present the application of GBS’s model to the prototype of the mini-halo source class, the Perseus cluster, and a new mini-halo candidate, Abell 2626, and discuss the physical implications of the results.

3.1. Observed mini-halos

The Perseus Cluster

We believe that the most striking evidence for electron re-acceleration in cooling flows is the case of the Perseus cluster (A426, $z=0.0183$). The diffuse radio emission from the mini-halo (see left panel in Fig. 1) has a total extension of $\sim 15'$ (at the redshift of the cluster $1'$ corresponds to ~ 30 kpc) and its morphology is correlated with that of the cooling flow X-ray map (Sijbring 1993; Ettori, Fabian & White 1998). Moreover, the mini-halo show a very steep spectrum (the integrated spectral index between $\nu = 327$ MHz and $\nu = 609$ MHz is $\alpha \sim 1.4$, Sijbring 1993) which steepens with distance from the center (see Fig. 2).

On smaller scales ($\sim 1'$), there is evidence of interaction between the radio lobes of the central radio galaxy 3C 84 and the X-ray emitting intracluster gas

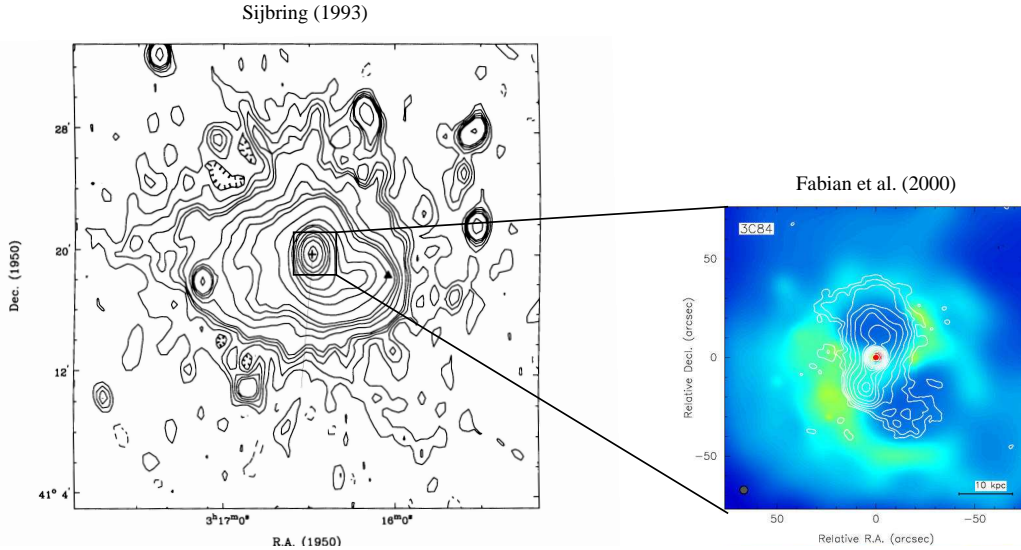


FIG. 1.— **Left panel:** 327 MHz map of the mini-halo in the Perseus cluster at a resolution of $51'' \times 77''$ (Sijbring 1993). The cross indicates the position of the cD galaxy NGC 1275. **Right panel:** X-ray (color)/radio (contours) overlay for the central part of the Perseus cluster around NCG 1275 (Fabian et al. 2000). X-ray data are obtained with *Chandra*. From Gitti et al. (2003).

(e.g. Böhringer et al. 1993; Fabian et al. 2000; see Fig. 1, right panel). A recent interpretation is that the holes in the X-ray emission are due to buoyant radio lobes which are currently expanding subsonically (Fabian et al. 2002). It is important to notice that the spectral index in these lobes ranges from ~ 0.7 in the center to ~ 1.5 in the outer regions (Pedlar et al. 1990), which is a value similar to the spectrum of the mini-halo extended over a scale ~ 10 times larger. Thus it is difficult to find a direct connection between the radio lobes and the mini-halo in terms of simple particle diffusion or buoyancy as, in this case, the diffusion time is considerably greater than the radiative lifetime of the radio electrons, while adiabatic losses during the expansion would cause a very rapid steepening of the spectrum preventing the detection of large-scale radio emission.

Thus, by assuming a primary origin for relativistic electrons in radio mini-halos, efficient re-acceleration mechanisms in the cooling flow region are necessary to explain the presence of the large-scale radio emission in Fig. 1.

Abell 2626

The cluster A2626 hosts a relatively strong cooling flow (White, Jones & Forman 1997) and contains an amorphous radio source near to the center (Roland et al. 1985; Burns 1990) which is extended on a scale comparable to that of the cooling flow region with an elongation coincident with the X-ray distribution (Rizza et al. 2000).

In order to extend the application of GBS’s model to this cluster, we have requested and analyzed some of the VLA archive data of A2626 with the aims of deriving the surface brightness map, the total spectral index and the spectral index distribution of the diffuse radio emission. Standard data reduction was done using the National Radio Astronomy Observatory (NRAO) AIPS package. In particular, we produced a 1.5 GHz map of the diffuse

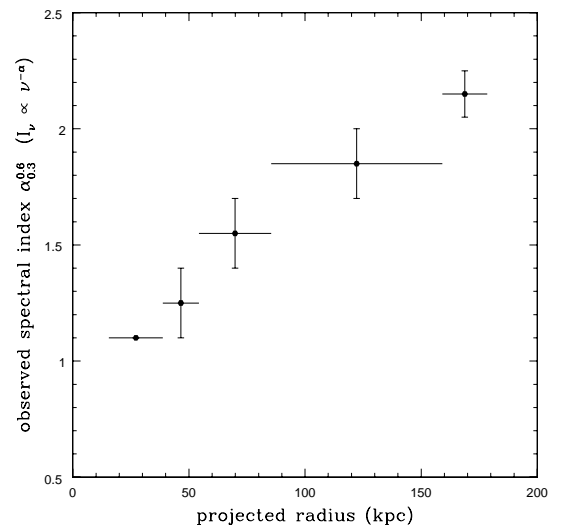


FIG. 2.— Radial spectral steepening observed in Perseus along the direction indicated in Fig. 1. Radio data are taken from Sijbring (1993).

radio emission after subtraction of the central discrete source (Fig. 3). To be conservative, the region in which the surface brightness is affected by the subtraction procedure (within the dashed circle in Fig. 3) has not been considered in the application of GBS’s model.

The integrated spectral index of the diffuse emission between $\nu = 330$ MHz and $\nu = 1.5$ GHz is $\alpha \sim 2.4$. By studying the spectral index distribution we found that, as in the case of Perseus, the diffuse radio emission shows a steep spectral index which steepens with the distance from the center (see Fig. 4).

The radio results are summarized in Table 1 (see Gitti

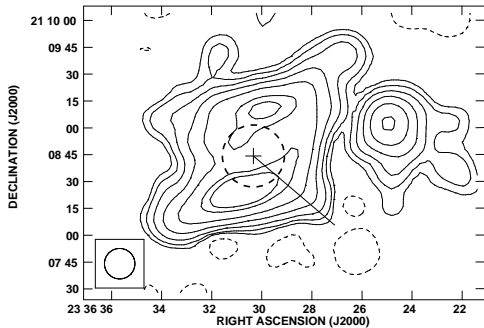


FIG. 3.— 1.5 GHz VLA map of A2626 at a resolution of $17'' \times 17''$ after the subtraction of the central discrete source indicated by the cross. The contour levels are -0.06 (dashed), 0.06 , 0.12 , 0.24 , 0.48 , 0.96 , 1.92 , 2.5 , 4 , 8 , 10 , 12 mJy/beam. The r.m.s. noise is 0.02 mJy/beam. The dashed line defines the region in which GBS’s model is not applicable, while the solid line represents the direction we have considered for the surface brightness profile (see Fig. 5).

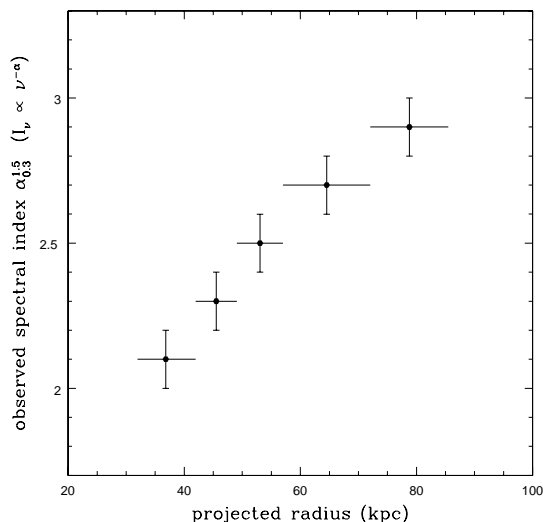


FIG. 4.— Radial spectral steepening observed in A2626 along the direction indicated in Fig. 3.

TABLE 1. RADIO RESULTS FOR A2626

Emission	S_{330} (mJy)	$S_{1.5}$ (mJy)	Size (arcsec ²)	α ($S_\nu \propto \nu^{-\alpha}$)
Nuclear	<9.3	13.5 ± 1	...	≤ -0.25
Diffuse	990 ± 50	29 ± 2	135×128	2.37 ± 0.05

et al. 2003 for a more detailed discussion).

The extended radio source observed at the center of A2626 is characterized by amorphous morphology, lack of polarized flux and very steep spectrum which steepens with distance from the center. Finally, the morphology of the diffuse radio emission is similar to that of the cooling flow region (Rizza et al. 2000). These results indicate that the diffuse radio source may be classified as a mini-halo.

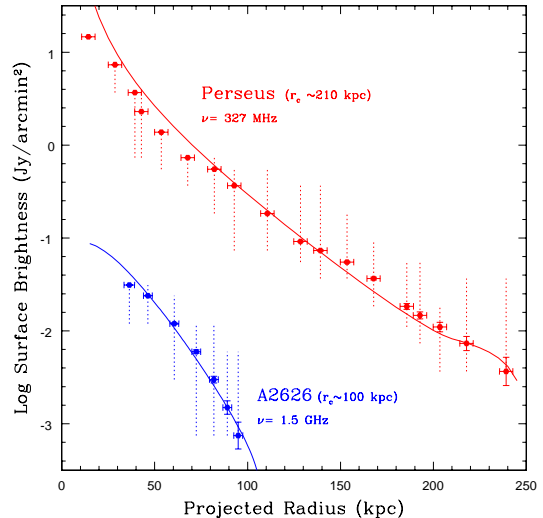


FIG. 5.— Fit to the surface brightness profile at 327 MHz for Perseus (in red) and 1.5 GHz for A2626 (in blue). Vertical bars represent the deviations from the spherical symmetry of the diffuse radio emission in other directions in the cluster with respect to the one we have considered (see Fig. 1 for Perseus and Fig. 3 for A2626).

3.2. Model application

In order to test the prediction of the model, we have calculated for both Perseus and A2626 the following expected observable properties:

- *total spectrum*: the total synchrotron spectrum is obtained by integrating the synchrotron emissivity from an electron population with the energy distribution given by Eq. 4 over the cluster volume, assumed to be spherical (we notice that the resulting spectrum in this model is weakly dependent on the radius of the sphere, and thus the assumption of spherical symmetry is reliable)
- *brightness profile*: the surface brightness profile expected by the model is obtained by integrating along the line of sight the synchrotron emissivity at a particular frequency
- *radial spectral steepening*: at varying projected radius, we obtain the surface brightness at different frequencies and then compute the spectral index.

The expected brightness profile and radial spectral steepening in the model are compared to the observed profiles along the radial direction indicated in Fig. 1 for Perseus and in Fig. 3 for A2626.

We found good results by assuming an isotropic compression of the magnetic field: in particular we notice that, by reproducing the observed brightness profile, the model is able to match the integrated spectrum and the radial spectral steepening as well. In Fig. 5, 6 and 7 we show the representative fits to the surface brightness profile, total spectrum and radial spectral steepening for Perseus (in red) and A2626 (in blue).

TABLE 2. DATA AND MODEL RESULTS FOR PERSEUS AND A2626

Cluster	X-RAY DATA				RADIO DATA		MODEL PARAMETERS			MODEL RESULTS			
	\dot{M} ($M_{\odot} \text{ yr}^{-1}$)	r_c (kpc)	kT (keV)	P_{CF} (erg s^{-1})	$P_{1.5}$ (W Hz^{-1})	r_{mh} (kpc)	B_c (μG)	$l_c/[\delta B_c/B_c]^2$ (pc)	s	$\gamma_{b,c}$	E_e (erg)	N_e	ϵ (%)
Perseus	519^{+3}_{-17}	210^{+100}_{-20}	$6.33^{+0.21}_{-0.18}$	2.6×10^{44}	4.4×10^{24}	~ 300	0.9–1.2	35–60	~ 2	1600	1.6×10^{58}	1.6×10^{61}	0.34
A2626	53^{+36}_{-30}	114^{+50}_{-59}	$3.1^{+0.5}_{-1}$	1.2×10^{43}	4.3×10^{23}	~ 100	1.2–1.6	120–180	~ -0.5	1100	2.2×10^{57}	3.2×10^{60}	0.69

NOTE. — Columns 2 and 3 list the cooling flow parameters, taken from Ettori, Fabian & White (1998) with the *ROSAT* PSPC for Perseus and from White, Jones & Forman (1997) with the *Einstein* IPC for A2626. Column 4 lists the average temperature of the ICM, taken from Allen et al. (1992) with *Ginga* for Perseus and from White, Jones & Forman (1997) with the *Einstein* IPC for A2626. Column 5 lists the power supplied by the cooling flow as estimated from X-ray data (see text). Columns 6 and 7 list the physical properties of the mini-halo: total power at 1.5 GHz and radius; radio data for Perseus are taken from Sijbring (1993). Columns 8, 9, and 10 list the parameters of the model derived by fitting all the observational constraints. Column 11, 12, and 13 list the physical properties derived by the model: respectively, the break energy of the electron spectrum at r_c , the energetics associated with the electrons re-accelerated in the cooling flow region and their total number. Column 14 lists the efficiency ϵ required for re-accelerating the relativistic electrons, given in percentage of P_{CF} taken from column 5. See text for details.

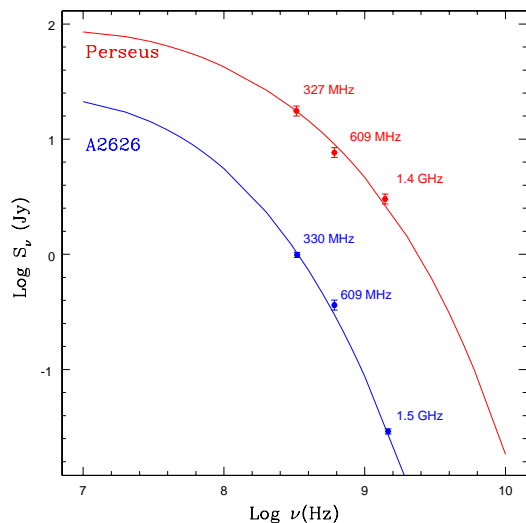


FIG. 6.— Fit to the total spectrum of the synchrotron emission for Perseus (in red) and A2626 (in blue). Radio data for Perseus are taken from Sijbring (1993). Radio data for A2626 are taken from Tab. 1, with the flux density at 609 MHz obtained by subtracting the estimated core emission from the total flux given by Roland et al. (1985).

3.3. Discussion

In this section we discuss the physical implications derived by applying GBS's model to Perseus and A2626. For completeness the X-ray and radio data as well as model results for these clusters are listed in Table 2.

It is worth pointing out that GBS's model is able to reproduce all the observational constraints of Perseus and A2626 for physically meaningful values of the parameters (Table 2). First of all, we found that the range of values obtained for B_c is in agreement with the measurements of magnetic field strengths in the ICM (Carilli & Taylor 2002 and references therein). We also point out that in the general theory of turbulent plasma one can calculate the wavelength which carries most of the turbulent energy in a spectrum of Alfvén waves (e.g. Tsytovich 1972). When applied to the case of the ICM, with standard values of the physical parameters, it gives results

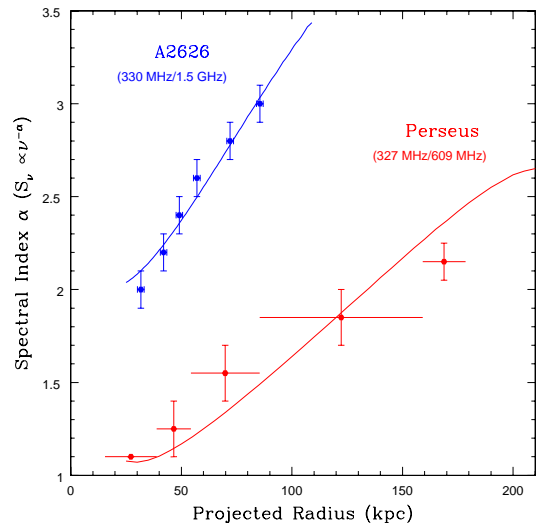


FIG. 7.— Fit to the spectral steepening with distance between $\nu = 327$ MHz and $\nu = 609$ MHz for Perseus (in red), and $\nu = 330$ MHz and $\nu = 1.5$ GHz for A2626 (in blue). Radio data for Perseus are taken from Fig. 2. Radio data for A2626 are taken from Fig. 4.

of the order of tens to hundreds of pc (GBS), thus the $l_c/[\delta B_c/B_c]^2$ values found in the model are reasonable.

The energetics associated with the population of electrons re-accelerated in the cooling flow region can be estimated as:

$$E_e \approx \frac{\pi r_c^3 e^2 m_e c^2 N(\gamma_b)_c \gamma_{b,c}^2}{(3-s)} \quad (5)$$

where $N(\gamma_b)_c$ is the number density (per unit γ) of electrons with energy $\gamma_b m_e c^2$ at r_c . The total number of relativistic electrons can be derived from the energetics as $N_e \sim 4E_e/(3m_e c^2 \gamma_{b,c})$.

It is worth noticing that both the energetics and the number of re-accelerated electrons estimated for A2626 are about one order of magnitude smaller than those found in Perseus. This is consistent with the fact that the radio power of the mini-halo in A2626 is about one order of magnitude smaller than that in Perseus (see column 6 of Table 2).

TABLE 3. OBSERVATIONAL DATA FOR MINI-HALOS

Cluster	z	\dot{M} ($M_{\odot} \text{ yr}^{-1}$)	kT (keV)	$P_{1.4}$ (W Hz $^{-1}$)
PKS 0745-191	0.1028	579^{+399}_{-215}	$8.3^{+0.5}_{-5.8}$	2.7×10^{25}
Abell 2390	0.2320	625^{+75}_{-75}	$9.5^{+1.3}_{-3.4}$	1.5×10^{25}
Perseus	0.0183	283^{+14}_{-12}	$6.3^{+1.5}_{-2.3}$	4.4×10^{24}
Abell 2142	0.0890	106^{+248}_{-106}	$11.4^{+0.8}_{-3.2}$	6.6×10^{23}
Abell 2626	0.0604	53^{+36}_{-30}	$3.1^{+0.5}_{-1.0}$	4.3×10^{23}

REFERENCES. — **X-ray data:** Perseus, A2142, A2626: White, Jones & Forman (1997) with the *Einstein* IPC; PKS 0745-191: White, Jones & Forman (1997) with the *Einstein* HRI; A2390: \dot{M} from Böhringer et al (1998) with the *ROSAT* PSPC, kT from White, Jones & Forman (1997) with the *Einstein* IPC. **Radio data:** PKS 0745-191: Baum & O’Dea (1991); A2390: Bacchi et al. (2003); Perseus: Sijbring (1993); A2142: Giovannini & Feretti (2000); A2626: Gitti et al. (2003).

The power P_e necessary to re-accelerate the emitting electrons, given by the minimum energy one must supply to balance the radiative losses of these electrons ($P_e \approx m_e c^2 \beta \gamma_{b,c}^2 \cdot N_e$, where β is the same as in Eq. 2) should be significantly smaller than the power supplied by the cooling flow. The maximum possible power P_{CF} which can be extracted from the cooling flow itself can be estimated assuming a standard cooling flow model and it corresponds to the $p dV/dt$ work done on the gas per unit time as it enters r_c : $P_{CF} = p_c \cdot 4\pi r_c^2 \cdot v_{F,c} \sim 2/5 L_{cool}$ (e.g. Fabian 1994, L_{cool} being the luminosity associated with the cooling region).

For both the clusters studied here, one finds that only a small fraction of P_{CF} should be converted into electron re-acceleration (see column 14 of Table 2), and thus we conclude that processes powered by the cooling flow itself are able to provide sufficient energy to power the radio mini-halos in Perseus and A2626.

For a more detailed discussion see Gitti et al. (2003).

4. Observational properties of mini-halos

We collected data from the literature and studied the observational properties of the population of radio mini-halos in relation with those of host clusters. The clusters in the sample were selected based on the presence of both a cooling flow and a diffuse radio emission with no direct association with the central radio source. In particular, since GBS’s model assumes a connection between the origin of the synchrotron emission and the cooling flow, to be conservative we selected those clusters where the size of the diffuse radio emission is comparable to the cooling radius.

Relevant X-ray and radio data are reported in Tab. 3, along with references, while in Fig. 8 we plotted the radio power at 1.4 GHz of the mini-halos versus the maximum power of cooling flows. A general trend is found, with the strongest radio mini-halos associated with the most powerful cooling flows.

We notice that the maximum powers which can be extracted from cooling flows are orders of magnitude larger

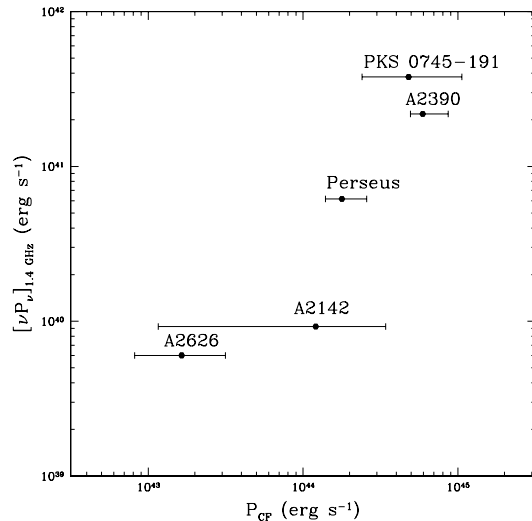


FIG. 8.— Integrated radio power at 1.4 GHz, $[\nu P_{\nu}]_{1.4\text{GHz}}$, vs. cooling flow power, $P_{CF} = \dot{M}kT/\mu m_p$, for the mini-halo clusters in Tab. 3.

than the integrated radio powers (see Fig. 8), in qualitative agreement with the very low efficiencies calculated in the model (see column 14 of Table 2).

As already discussed in Sect. 2, it is worth noticing that new *Chandra* and *XMM-Newton* results obtained for a limited number of objects hint to an overestimate of \dot{M} derived by earlier observations: in particular, the consensus reached in these studies (e.g. McNamara et al. 2000; Peterson et al. 2001; David et al. 2001; Molendi & Pizzolato 2001; Böhringer et al 2001; Peterson et al. 2003) is that the spectroscopically derived cooling rates are a factor ~ 5 -10 less than earlier *ROSAT* and *Einstein* values (e.g. Fabian & Allen 2003). This factor seems to be similar for all clusters in a large range of \dot{M} , giving a systematic effect that will not spoil the correlation reported in Fig. 8.

We can conclude that even by considering reduced spectroscopically derived \dot{M} , the cooling flow powers are well above the radio powers emitted by mini-halos, therefore even if the cooling flow was partially re-heated and stopped, the basic idea and results of the model would not change.

M. G. would like to thank F. Brighenti for stimulating discussion during the Conference and S. Dall’Osso for his constant help and insightful comments. M. G. and G. B. acknowledge partial support from CNR grant CNRG00CF0A. This work was partly supported by the Italian Ministry for University and Research (MIUR) under grant Cofin 2001-02-8773 and by the Austrian Science Foundation FWF under grant P15868.

References

- Allen, S. W., Fabian, A. C., Johnstone, R. M., Nulsen, P. E. J., & Edge, A. C. 1992, *MNRAS*, 254, 51
- Bacchi, M., Feretti, L., Giovannini, G., & Govoni, F. 2003, *A&A*, 400, 465
- Baum, S. A., & O'Dea, C. P. 1991, *MNRAS*, 250, 737
- Böhringer, H., Voges, W., Fabian, A. C., Edge, A. C., & Neumann, D. N. 1993, *MNRAS*, 264, L25
- Böhringer, H., Tanaka, Y., Mushotzky, R. F., Ikebe, Y., & Hattori, M. 1998, *A&A*, 334, 789
- Böhringer, H., Belsole, E., Kennea, J., Matsushita, K., Molendi, S., et al. 2001, *A&A*, 365, 181
- Brunetti, G., Setti, G., Feretti, L., & Giovannini, G. 2001, *MNRAS*, 320, 365
- Burns, J. O. 1990, *AJ*, 99, 14
- Carilli, C. L., & Taylor, G. B. 2002, *ARA&A*, 40, 319
- David, L. P., Nulsen, P. E. J., McNamara, B. R., Forman, W., Jones, C., et al. 2001, *ApJ*, 557, 546
- Edge, A. C., 2001, *MNRAS*, 328, 762
- Edge, A. C., Stewart, G. C., Fabian, A. C. 1992, *MNRAS*, 258, 177
- Ettori S., Fabian A. C., & White, D. A. 1998, *MNRAS*, 300, 837
- Fabian, A. C. 1994, *ARA&A*, 32, 277
- Fabian, A. C., Nulsen, P. E. J., & Canizares, C. R. 1984, *Nature*, 310, 733
- Fabian, A. C., Sanders, J. S., Ettori, S., Taylor, G. B., Allen, S. W., et al. 2000, *MNRAS*, 318, 65
- Fabian, A. C., Celotti A., Blundell, K. M., Kassim, N. E., & Perley, R. A. 2002a, *MNRAS*, 331, 369
- Fabian, A. C., & Allen, S. W. 2003, to appear in the Proceedings of the XXI Texas Symposium on Relativistic Astrophysics held on December 9–13 2002, in Florence, Italy [astro-ph/0304020]
- Feretti, L., & Giovannini, G. 1996, *IAUS*, 175, 333
- Ge, J. P., & Owen, F. N. 1993, *AJ*, 105, 3
- Giovannini, G. & Feretti, L. 2000, *NewA*, 5, 335
- Giovannini, G. & Feretti, L. 2002, in *Merging Processes in Clusters of Galaxies*, ed. L. Feretti, I. M. Gioia, G. Giovannini (Dordrecht: Kluwer)
- Gitti, M., Brunetti, G., & Setti, G. 2002, *A&A*, 386, 456 (**GBS**)
- Gitti, M., Brunetti, G., Feretti, L., & Setti, G. 2003, *A&A* submitted
- McNamara, B. R., Wise, M., Nulsen, P. E. J., David, L. P., Sarazin, C. L., et al. 2000, *ApJ*, 534, L135
- Melrose, D. B. 1980, *Plasma Astrophysics: Nonthermal Processes in Diffuse Magnetized Plasmas*, Gordon and Breach
- Molendi, S., & Pizzolato, F. 2001, *ApJ*, 560, 194
- Pedlar, A., Ghataure, H. S., Davies, R. D., et al. 1990, *MNRAS*, 246, 477
- Peterson, J. R., Paerels, F. B. S., Kaastra, J. S., Arnaud, M., Reiprich, T. H., et al. 2001, *A&A*, 365, 104
- Peterson, J. R., Kahn, S. M., Paerels, F. B. S., Kaastra, J. S., Tamura, T., et al. 2003, *ApJ*, 590, 207
- Pfrommer, C., & Enßlin, T. 2003, *A&A* in press [astro-ph/0306257]
- Rizza, E., Loken, C., Bliton, M., Roettiger, K., & Burns, J. O. 2000, *AJ*, 119, 21
- Roland, J., Hanish, R. J., Véron, P., & Fomalont, E. 1985, *A&A*, 148, 323
- Salomé, P., & Combes, F., 2003, astro-ph/0309304
- Sarazin, C. L. 2002, in *Merging Processes in Clusters of Galaxies*, eds. L. Feretti, I. M. Gioia, G. Giovannini (Dordrecht: Kluwer)
- Sijbring, D. 1993, Ph.D. Thesis, Groningen
- Soker, N., & Sarazin, C. L. 1990, *ApJ*, 348, 73
- Tribble, P. C. 1993, *MNRAS*, 263, 31
- Tsyтович, V. N. 1972, *An introduction to the Theory of Plasma Turbulence* (Pergamon Press)
- White, D. A., Jones, C., & Forman, W. 1997, *MNRAS*, 292, 419